6.2 Potential Vorticity Front in a Channel

To Do: Johnson et al. use α to denote the background flow, whereas U_o was used in the previous section. Should I change to U_o ?

One of the simplest models for exploring the physics associated with potential vorticity gradients is based on a material contour separating two regions of different, uniform potential vorticity. The following development is due to Haynes et al. (1994) and Johnson and Clarke (1999, 2001), who considered the situation in which the potential vorticity front is confined to a channel with a mean flow. In a certain sense, the model is what would be obtained from the channel problem of Sec. 2.9 if the gravity mode is eliminated (using a rigid lid) and the number of potential vorticity modes is reduced to one.

Consider a zonal channel occupying $0<y^*<w^*$ and containing a homogeneous flow capped by a rigid lid. The statement of conservation of potential vorticity is given by (6.1.8), with

$$d^*=D-h^*(x^*,y^*). \tag{6.2.1}$$

Although β^* is taken as zero, variations in ambient potential vorticity will arise due to variations in h^*. It is assumed that such variations are weak ($h^*<<D$) and, therefore, that the horizontal velocity is approximately nondivergent:

$$\nabla\cdot(\mathbf{u}^*)=0\,.$$

In this case a streamfunction ψ^* exists, with $v^*=\partial\psi^*/\partial y^*$, $u^*=-\partial\psi^*/\partial x^*$, even though the velocity is not geostrophically balanced. Under these conditions the shallow water potential vorticity can be approximated as

$$\frac{f_o+\xi^*}{d^*}\cong\frac{f_o}{D}+\frac{f_o h^*}{D^2}+\frac{\xi^*}{D}=\frac{f_o}{D}+\frac{f_o h^*}{D^2}+\frac{\nabla^2\psi^*}{D}. \tag{6.2.2}$$

Suppose that the bottom topography consists a topographic step:

$$h^*=\begin{cases}0 & (y^*>Y_h^*(x^*))\\ \delta h^* & (y^*<Y_h^*(x^*))\end{cases}, \tag{6.2.3}$$

where $\delta h^*/D<<1$. The shallow fluid lying on the shelf to the 'right' side of the channel (facing positive x^*) implies relatively high potential vorticity there, at least in the absence of other vorticity gradients. (This configuration reverses the usual situation on a beta plane, where high potential vorticity occurs to the north.) The jump in potential vorticity across the step gives rise to a class of waves closely related to topographic Rossby waves (Section 2.1). These waves propagate forward (towards positive x^*) but can be arrested if a negative mean flow is added. For example, if step lies at mid-channel $Y_h^*=w^*/2$ and a

uniform flow $u^*=-\alpha^*$ is present, the wave frequency ω^* is given in terms of the wave number k^* by

$$\omega^* = -k^*\alpha^* + \frac{f_o \delta h^*}{2D}\tanh[\tfrac{1}{2}k^* w^*] \qquad (6.2.4)$$

(see Exercise 1). Short waves ($k^*<<1$) are therefore advected downstream at the speed α of the background flow. Long waves ($k^*w^*<<1$) have speed $c^*=\omega^*/k^* \rightarrow -\alpha^* + 1/4 f_o \delta h^* w^*/D$ and are brought to rest when $\alpha^*=1/4 f_o w^* \delta h^*/D$. For smaller α^* stationary, dispersive waves with downstream group velocity exist. At higher speeds, all linear disturbances are swept downstream.

We wish to consider the effects of variations in the position Y_h^* of the step. Attention will be confined to cases where Y_h^* experiences an isolated narrowing of the shelf, centered at $x^*=0$ (Figure 1). Far upstream and downstream, it will be assumed that the step lies at channel midpoint ($Y_h^* \rightarrow 1/2$). In addition, the flow is assumed to be initially quiescent, so that the perturbation potential vorticity $(\Delta^2\psi^*/D) + (f_o h^*/D^2)$ is initially zero on the deeper side of the channel ($y^* > Y_h^*(x^*)$) and has value $f_o \delta h^*/D^2$ on the shallower side ($y^* < Y_h^*(x^*)$). At $t^*=0^+$, a uniform velocity $u^*=-\alpha^*$ is imposed, causing some fluid to cross the step, carrying with it its initial potential vorticity. The material contour or 'front' $y^*=Y^*(x^*,t^*)$ separating the low and high potential vorticity no longer coincides with the position of the topographic step. The potential vorticity distribution at any time is given by

$$\frac{\Delta^2\psi^*}{D} + \frac{f_o \delta h^*}{D^2}\begin{Bmatrix} 0 & (y^* > Y_h^*(x^*)) \\ 1 & (y^* < Y_h^*(x^*)) \end{Bmatrix} = \begin{Bmatrix} 0 & (y^* > Y^*(x^*,t^*)) \\ f_o \delta h^*/D^2 & (y^* < Y^*(x^*,t^*)) \end{Bmatrix}.$$

It is important to realize at the outset that total transport in the channel must remain fixed as the flow evolves. This property can be deduced from the condition of no normal flow along the channel side walls, which requires that ψ^* be uniform there. Although the side-wall values of ψ^* can generally vary with time, this is precluded by the nature of the initial value problem posed above. The flow at $y \rightarrow \pm\infty$ remains fixed in time since disturbances generated by variations in Y_h^* propagate upstream and downstream at finite speed. The boundary values of ψ^* and hence the total volume flux therefore remain fixed. Other transports including that of potential vorticity may be altered.

If variables are nondimensionalized using w^*, $D/f_o\delta h^*$ and $\delta h^* f_o w^*/D$ as horizontal length, time and velocity scales (the topographic equivalent of L, L/β, and βL^2), the previous relation becomes

$$\nabla^2\psi = \begin{Bmatrix} 0 & (y > Y(x,t)) \\ 1 & (y < Y(x,t)) \end{Bmatrix} - \begin{Bmatrix} 0 & (y > Y_h(x)) \\ 1 & (y < Y_h(x)) \end{Bmatrix}. \qquad (6.2.5)$$

Initially shallow(deep) fluid that crosses the step into the deeper(shallower) region will be stretched(squashed) and its relative vorticity will be incremented by an amount +1(-1). The fluid vorticity is therefore piecewise constant as shown in Figure 6.2.1b. Solutions to (6.2.5) in the three regions can be matched by requiring that ψ remain continuous across the boundaries of the regions. The potential vorticity front itself is a material boundary and its motion obeys the kinematic relation $v = \frac{\partial \psi}{\partial x} = \frac{\partial Y}{\partial t} + u(x,Y,t)\frac{\partial Y}{\partial x}$, which can also be expressed as

$$\frac{\partial Y}{\partial t} = \frac{d}{dx}\psi(x,Y(x,t),t) \qquad (6.2.6)$$

With the present scaling, the Rossby number U/f_oL becomes $\delta h^*/D$, which is <<1 by prior assumption. The velocity is therefore geostrophically balanced and the model can be considered quasigeostrophic but with an essentially infinite Rossby radius of deformation (i.e. S=0 in 6.1.6).

(b) Long-wave behavior.

In the usual manner of hydraulic analysis we begin by considering the long wave behavior of the flow induced when the along-channel variations of the step position are gradual in comparison with cross-channel variations. We therefore let

$$Y_h = \tfrac{1}{2} - \varepsilon \mathrm{sech}^2(\tilde{x}) \qquad (6.2.7)$$

where $\tilde{x} = \mu^{1/2}x$ and μ<<1. In addition, the stream function is composed of the contribution from the background velocity $-\alpha$ imposed at t=0$^+$ plus the residual ϕ:

$$\psi = \alpha y + \phi(\tilde{x},y,\tilde{t}), \qquad (6.2.8)$$

where $\tilde{t} = \mu^{1/2}t$. [The slow time variable associated with gradual variations in the x-direction is suggested by (6.2.6).]

Equation (6.2.5) now becomes

$$\frac{\partial^2\phi}{\partial y^2} + \mu\frac{\partial^2\phi}{\partial \tilde{x}^2} = \begin{Bmatrix} 0 & (y > Y(\tilde{x},\tilde{t})) \\ 1 & (y < Y(\tilde{x},\tilde{t})) \end{Bmatrix} - \begin{Bmatrix} 0 & (y > Y_h(\tilde{x})) \\ 1 & (y < Y_h(\tilde{x})) \end{Bmatrix} \qquad (6.2.9)$$
$$= H(y - Y_h(\tilde{x})) - H(y - Y(\tilde{x},\tilde{t}))$$

where $H(y)$=1 for $y>0$ and $H(y)$=0 for y<0. The boundary conditions $\psi=0,\alpha$ at y=0,1 imply

$$\phi(\tilde{x},0,\tilde{t}) = \phi(\tilde{x},1,\tilde{t}) = 0 \qquad (6.2.10)$$

For small μ the solution to (6.2.9) subject to (6.2.10) may be written as

$$\phi = \tfrac{1}{2}(y-Y_h)^2 H(y-Y_h) - \tfrac{1}{2}(y-Y)^2 H(y-Y) + \tfrac{1}{2}\left[(1-Y)^2 - (1-Y_h)^2\right]y$$
$$-\frac{\mu}{12}\frac{\partial^2}{\partial\tilde{x}^2}\{\tfrac{1}{2}(y-Y_h)^4 H(y-Y_h) - \tfrac{1}{2}(y-Y)^4 H(y-Y) +$$
$$((1-Y)^2 - (1-Y_h)^2)(y^3 - y) + \tfrac{1}{2}\left[(1-Y)^4 - (1-Y_h)^4\right]y\} + O(\mu^2)$$

and (6.2.6) then gives

$$\frac{\partial Y}{\partial\tilde{t}} = \frac{\partial}{\partial\tilde{x}}\psi_h(Y,Y_h) + \frac{\mu}{6}\frac{\partial}{\partial\tilde{x}}\Big\{(Y-Y_h)^2 H(Y-Y_h)\left(\frac{\partial^2 Y_h}{\partial\tilde{x}^2}(Y-Y_h) - 3\left(\frac{\partial Y_h}{\partial\tilde{x}}\right)^2\right)$$
$$-Y\left[\frac{\partial^2 Y_h}{\partial\tilde{x}^2}(1-Y_h)(Y^2 - 1 + (1-Y_h)^2) - \left(\frac{\partial Y_h}{\partial\tilde{x}}\right)^2 (Y^2 - 1 + 3(1-Y_h)^2\right] \qquad (6.2.11)$$
$$-2Y(1-Y)\frac{\partial}{\partial\tilde{x}}[Y(1-Y)\frac{\partial Y}{\partial\tilde{x}}]\Big\} + O(\mu^2)$$

where

$$\psi_h(Y,Y_h) = \alpha Y + \frac{1}{2}(Y-Y_h)^2 H(Y-Y_h) + \frac{1}{2}\left[(1-Y)^2 - (1-Y_h)^2\right]Y. \qquad (6.2.12)$$

In the long-wave limit the O(μ) terms (6.2.11) are neglected, leaving the hyperbolic equation

$$\frac{\partial Y}{\partial\tilde{t}} - \frac{\partial\psi_h}{\partial Y}\frac{\partial Y}{\partial\tilde{x}} = \frac{\partial\psi_h}{\partial Y_h}\frac{\partial Y_h}{\partial\tilde{x}}. \qquad (6.2.13)$$

Long-wave disturbances therefore propagate at the characteristic speed

$$c = -\frac{\partial\psi_h(Y,Y_h)}{\partial Y}. \qquad (6.2.14)$$

In the absence of variations in Y_h the value of Y is conserved following this speed. The presence of just one wave is another point of departure from the types of problems we have been studying. There have typically been two waves with speeds, c_+ and c_-, and the flow has been labeled supercritical or subcritical according to $c_+c_- > 0$ or $c_+c_- < 0$. Here the

flow will be called supercritical if $c<0$; that is, if wave propagation is in the same direction as the background flow. For the initial upstream state ($Y=Y_h=0$), c reduces to $1/4-\alpha$ and therefore this flow is supercritical when $\alpha>1/4$. A Froude number for this upstream flow can therefore be defined by

$$F_o = 4\alpha = \frac{4\alpha^* D}{f_o \delta h w^*},$$

which can be considered a form of $U/\beta L^2$ if $U=\alpha^*$, $L=w^*$, and $\beta^*=f_o\delta h/Dw^*$.

If the flow is steady the potential vorticity front is a streamline, $\psi=\psi_o$ say, and the position of the front is determined by

$$\psi_h(Y, Y_h) = \psi_o .$$

The function $\psi_h(Y, Y_h) - \psi_o$ may be treated as Gill's $\mathcal{G}$ and the critical condition $\partial\mathcal{G} / \partial\tilde{x} = 0$ is clearly equivalent to $c=0$. Figure (6.2.2) contains a selection of contour plots of $\psi_h(Y, Y_h)$ for various values of the initial flow speed (or equivalently the total transport) α. In the absence of jumps or other dissipative features, solutions must lie along the contours. A solution originating from an upstream condition $Y=Y_h=1/2$ must lie along the contour that passes through the center of the plane and the corresponding contour value is $\psi_o=-\alpha/2$. The segments of contours with positive tilt correspond to subcritical $c>0$ flow, while negative tilts correspond to supercritical flow. Maxima or minima in Y_h along a contour correspond to critical flow and it can be seen the curves have zero, one or two such extremes. Although the presence of two extremes suggests the possibility of two control sections within the same solution, one would involve a supercritical-to-subcritical transition subject the instability described in Section 1.4. Still, the presence of two extremes makes for a richer variety of possible steady flow configurations. *It is also interesting that the potential vorticity-controlled solutions of Pratt and Armi had single extreme. Perhaps this fundamental difference lies in the fact that the potential vorticity gradient in their case is continuous, but it would be good to get Ted Johnson's opinion on this.*

Now consider some examples in which the position of the step is given by (6.2.7). Fix the amplitude ε of the excursion of the step at 0.15 and consider a sequence of initial value problems with progressively larger transports: α =0.05, 0.1,0.15, and 0.3. (The corresponding initial upstream Froude numbers are 0.2, 0.4, 0.6, and 1.2.) The families of possible steady solution curves corresponding to these transports are shown in Figures 6.2.3a,c,e,g. The potential vorticity front initially coincides with the step but could evolve to some other steady state as $t\rightarrow\infty$. The expected final state for each case is indicated by a thick line overlaid on the contours and a plan view showing the corresponding front and step positions appears in the figure to the right (6.2.3b,d,f, or h). In some cases the position Y_∞ of the front far upstream is unchanged from its initial value ($Y_\infty=0$); that is, no upstream influence exists. In other cases this upstream state is altered. The final steady states can be grouped into four classes:

Type S: Subcritical flow (α=*.05, so* F_o=0.2) Referring to figure 6.2.3a, we attempt to construct a steady solution beginning upstream (Y=Y_h=1/2) corresponding to the very center of the contour plot. The tilt of the contour that passes through this point is positive, so the flow is subcritical. The solution over the remainder of the channel lies along an S-shaped curve that passes through this point. Proceeding downstream from the origin, this curve is traced in the lower left direction as Y_h decreases, as suggested by the solid line in the figure. When the minimum Y_h is passed the solution is retraced back to the origin. The result is a symmetrical, subcritical solution (Frame b).

Type CC: Flow controlled at the contraction: (α=*.1 so* F_o=0.4) Here the larger value of α causes the excursions of the *S*-shaped curves to decrease. If one proceeds as in the first case, tracing along the curve that passes through the origin, the lower extreme of this curve is reached before the maximum step amplitude is encountered. Since it is impossible to continue along the same curve, we must assume that the upstream condition is no longer valid. Proceeding as in earlier examples of this type, we find the new value of Y_∞ by demanding that the flow be critical at the crest (Y_h=.35) of the step. The appropriate solution curve has an extrema at this value and is shown as a thick segment in Figure 2c. The full solution is then constructed by tracing that curve along its subcritical branch upstream and along the supercritical branch downstream (vice versa would lead to an unstable flow). This trace is shown in Frame c and the corresponding solution in Frame d. The new value of Y_∞ for this solution is >1/2, meaning that the upstream position lies on the deeper side of the step.

Type AC: Approach control with supercritical leap: (α=.15, *so* F_o=0.6) If α is further increased the topography of the solution plane can change to the point where a contraction controlled solution is no longer viable (see Frame 2e). One begins as in the previous example by assuming the flow is critical where Y_h reaches it minimum value, in this case 0.35. The presumptive solution lies along the contour that achieves a minimum in Y_h at this value, and this is indicated by a dashed line in Figure 2e. However, trouble arises when one attempts to trace the subcritical branch of this curve upstream. A maximum in Y_h is encountered before the upstream value (Y_h=0.5) is reached. The solution cannot be continued beyond this point. Direct solution of the initial value problem for this case suggests a new type of steady solution in which the upstream flow itself is critical (akin to 'approach control' of two-layer flow, as discussed in Chapter 5.) The corresponding solution contour has an maxima at Y_h=0.5. If one proceeds downstream, a decision must be made as to which branch of the curve to follow. Selection of the subcritical branch would give rise to an unstable situation in which disturbances generated downstream would propagate upstream, only to encounter and approaching critical flow. The same accumulation of disturbance energy that marks a supercritical-to-subcritical transition would be in play. Selection of the supercritical branch avoids this difficulty and we therefore trace along this branch as the crest of the topography is passed. This trace is indicated by arrows along the solid line in Figure 6.2.3e. However, continuing downstream would require retracing the supercritical branch of the curve back to the extrema, so that the downstream flow would also be critical and

the instability mentioned above would come into play. In fact, direct simulations show that the solution jumps to the other supercritical branch of the S-shaped curve, as suggested in the figure. This jump is called a supercritical leap and the corresponding solution is shown in Figure 6.2.3f. There is a range of possible Y_h values at which the leap can occur and the true value can ascertained using by jump conditions, to be discussed later.

Type SR: Supercritical flow: (α=*.3 so* F_o=1.2) If the transport is strong enough, the *S*-shape character of the solution curves is lost and only supercritical flow is possible. Here solutions with no upstream influence are easily constructed. A typical example is shown in Figures 6.2.3g,h.

For given α (or equivalently F_o), the predicted steady solution depends upon the value of ε as described in the previous examples. Analysis of the function $\psi_h(Y, Y_h)$ allows one to determine the boundaries between the four different flow regimes and these boundaries are indicated in Figure 2.3. Keep in mind that the initial upstream flow is critical (F_o=1) when α=1/4. It is notable that flows with approach controls (AP) occupy a relatively large region of the parameter space. If the upstream position of the step is not at midchannel, then the regime diagram is different. A key difference is the emergence of the fifth type of steady flow, the *twin supercritical leap*. These features are discussed by Johnson and Clarke (1999).

(c) Simulations based on contour dynamics.

Haines et al. (1994) verified the above solutions by solving the initial value problem of the unapproximated potential vorticity equation (6.2.5) using the method of contour dynamics[1] (CD). The governing equation and procedure are very similar to those introduced in Section 3.2 and a sample of results is shown in Figures 6.2.4-6.2.7. In all cases the dashed line represents the steady solution that would be obtained by the above long wave theory.

Two examples of flow developing from initial conditions in the subcritical region of Figure 3 are shown in Figure 6.2.4. The position Y_h of the step and the predicted steady long wave solution are shown along with the result of the CD simulation as it nears a steady state. In (a) the variation in Y_h is very gradual and the final steady solution resembles that of Figure 6.2.3a. The main departure is the presence of small lee waves in the CD simulation. In (b) the same initial conditions and step excursion ε are used but the scale of variation of Y_h is shorter and, in fact, well outside the long-wave approximation. The scale of topographic variations in this case is closer to the scale of the lee waves, and the latter are more efficiently generated.

[1] The procedure is similar to that described in Section 3.3. The Green's function continues to be that defined by (3.2.13) but the potential vorticity distribution is complicated by the presence of the topographic step.

Solutions with a contraction control can be generated if the value of ε is increased sufficiently. The resulting upstream influence leads to an increase in Y_∞ above its value of 0.5. The characteristic wave speed in this situation increases with increasing Y and thus the disturbance is a rarefaction (Exercise 4)]. These expectation are born out in CD simulations (Figure 6.2.5) that also exhibit prominent short wave effects in the lee of the contraction. In Frame (a), which shows a case of gradually varying Y_h, an undular bore develops in the lee of the contraction. It can be seen propagating slowly downstream. The leading wave crest is close to the point of pinching off and forming a detached eddy. In (b) the topographic feature has been shortened with the result that the undular bore has been replaced by nearly discontinuous bore, again propagating downstream slowly. A counterclockwise eddy has been ejected from the downstream portion.

The establishment of a flow with an approach control (Figure 6.2.6) begins in a similar manner (Figure 6.2.6a). A rarefaction wave is generated at the contraction and this disturbance moves upstream, increasing the value of Y_∞. In the contraction itself, the flow undergoes a subcritical-to-supercritical transition and a downstream bore develops. So far the evolution is similar to the previous case. However, the region of flow just upstream of the contraction begins to evolve in a new manner, as evidenced by a steepening of the front into an abrupt bend (Frame b). Although the bend first forms upstream of x=0, it slowly moves downstream and settles into a fixed position (frame c). The final steady state (Frame c) can be compared to the long-wave solution (thicker line) obtained by introducing a supercritical leap highest value of x for which it can occur. It is notable that the supercritical leap calculated using CD is smooth and shows no signs of turbulence or energy dissipation, suggesting the energy conservation could be a basis for the formulation of the jump condition. We return to this topic later.

(d) Dispersion

The CD simulations reveal the presence of lee waves, undular bores, supercritical leaps, and other features that lie outside of the realm of long-wave theory. An advantage of the present model is that these dispersive, short-scale effects can be explored with relative ease. One way to gain some insight is to include the previously neglected $O(\mu)$ corrections to the streamfunction in (6.2.11). It will be convenient to switch back to the original coordinates, with x and t replacing $\tilde{x} / \mu^{1/2}$ and $\tilde{t} / \mu^{1/2}$, but the reader should keep in mind that the resulting expressions are approximations, valid to $O(\mu)$.

One of the most important elements added by dispersion is the ability of disturbances of finite scale to remain stationary in the flow. If the position of the step is held constant, these disturbances are governed by the steady form of (6.2.11) with fixed Y_h. Integration of this relation respect to x yields

$$\psi_h(Y, Y_h) - \frac{1}{3} Y(1-Y) \frac{d}{dx}[Y(1-Y)\frac{dY}{dx}] = \psi_o,$$

where ψ_o is a constant. In contrast to the previous analysis, the upstream flow is not constrained to be parallel. Multiplication of this relation by $\partial Y/\partial x$ and integration with respect to x leads to

$$\frac{1}{6}Y^2(1-Y)^2\left(\frac{dY}{dx}\right)^2 + V(Y,Y_h) = M, \qquad (6.2.15)$$

where M is a constant and

$$V(Y,Y_h) = \psi_o Y - \tfrac{1}{2}\left[\alpha + Y_h - \tfrac{1}{2}Y_h^2 + \tfrac{1}{4}Y^2 - \tfrac{2}{3}Y\right]Y^2 - \tfrac{1}{6}(Y-Y_h)^3 H(Y-Y_h).$$

Solutions to (6.2.15) are represented by contours of constant M in the 'phase space' $(Y, \partial Y/\partial x)$. As an example, the contours for the case Y_h=0.5, α=0.1, and $\psi_o=\alpha/2$ are plotted in Figure 6.2.7a. There are three fixed points (0.5,0) and (0.5±.38,0) corresponding to parallel flows (Y=constant). The first of these corresponds to the upstream flow assumed in the initial value problem; the front lies at the position of the step and both are at mid-channel. Since α<1/4, this flow is subcritical. The surrounding closed orbits represent periodic stationary waves. The small orbits in the immediate vicinity of the fixed point are essentially the linear stationary waves corresponding to ω^*=0 in 6.2.4. As one moves away from the fixed point the wave amplitude increases until a heteroclinic trajectory joining the remaining fixed points is reached. Both points represent uniform supercritical flows, a fact that can be shown directly from (6.2.14) or deduced from the property that they support no small amplitude stationary waves. The trajectories that join the two points corresponds to solutions for which Y varies monotonically over $-\infty<x<\infty$ from one supercritical state to the other (Figure 6.2.7b). The solution is sometime referred to as a *kink soliton*. Since the supercritical leap shown in Figure 6.2.6c occurs over such a small interval in x, the change in Y_h from one side of the leap to the other is relatively small. For this reason, the kink soliton can be regarded as an approximation to a leap[2].

Although the phase plane solutions are valid for a fixed step position, one can anticipate the effect of a gradually varying Y_h by allowing the actual solution trajectory to gradually move from one contour to the next in Figure 6.2.7a. As an example, consider a a solution that is subcritical and parallel far upstream of the shelf contraction. The upstream state therefore corresponds to the subcritical fixed point in Frame (a). As one moves downstream and encounters the region of variable Y_h the solution moves away from the fixed point, crossing the closed orbits. Downstream, where Y_h returns to its upstream value of 0.5, the solution remains one of the closed orbits. Each orbit has a different value of M, which can be interpreted as the momentum flux of the solution (Johnson and Clarke, 2001). The change in M from the fixed point to the final closed

[2] Note, however, that the kink soliton of Figure 6.2.7b does not represent the supercritical leap of Figure 6.2.6c.

orbit is due to wave drag (form drag) occurring in the constriction. This drag generally is at its greatest when the x-scale of the topography is comparable to the wave length of lee waves and this can result in a downstream orbit that lies quite far from the subcritical fixed point. For the solution shown in Figure 6.2.4a Y_h varies gradually (μ is <<1) and the lee waves are small, corresponding to orbits close to the fixed point. In Figure 6.2.4b, where μ is O(1), the lee wave orbits are larger.

In some cases, the form drag may be sufficient to force the solution to cross the heteroclinic trajectory in Figure 6.2.4a, so that the downstream flow lies on an open trajectory. The latter do not represent acceptable end states since they lead to unbounded values of Y far downstream. In this case an upstream disturbance must be generated, altering the value of ψ_o and leading to a new phase plane with an expanded heteroclinic orbit. Dispersion can thereby lead to a hydraulically controlled solution even though a perfectly valid subcritical, long-wave solution exists. If the step does not lie at mid-channel, the symmetry of the phase plane is lost and the supercritical fixed points are no longer connected. Some of the consequences are explored in Exercise 6.

In order to make more explicit consideration of the effects of variations in Y_h in the presence of dispersion, one can integrate the full steady version of (6.2.11) beginning with a given upstream state. One of the difficulties in doing so is that wavy upstream states are now possible and there is no obvious reason to reject them. This matter can be handled more cleanly by solving the full initial value problem using the full time dependent version of (6.2.11). As reported by Johnson and Clarke (2001), the typical steady state solution that develops is a dispersion modified version of the expected long-wave solution. Among the effects of dispersion are the presence of lee waves or downstream undular bores, and the smoothing of features like supercritical leaps that are represented in the long-wave limit by discontinuities. The function $Y(x,t)$ is constrained to be single valued in x and therefore wave breaking or eddy pinching is not allowed. Solutions for values of α and ε that lie within the subcritical (S) portion of the regime diagram (Figure 6.2.3), but close to the boundary with CC, can evolve to hydraulically controlled flows of the AC type if μ is sufficiently large. The loss of the subcritical solution suggested above is thereby confirmed. Another consequence of dispersion is the failure in certain small regions of the (α,ε) parameter space for the solution to settle into steady state.

In flows with continuous variations in potential vorticity or other complexities, the hydraulic problem with dispersion becomes less tractable. In such cases, progress can be made by assuming that the topographic variations (here measures by ε) are small and that the initial flow is close to the critical speed. The proximity to criticality means disturbances can be resonantly excited by variations in topography. Weak nonlinearity and dispersion act at finite amplitude to limit growth and the resulting finite amplitude disturbances can be interpreted as hydraulic transitions, lee waves, and undular or monotonic jumps and bores. Solutions bear some similarity to the cases just discussed. The precise form of the evolution equation depends on the character of the wave guide. If the flow has imposed transverse scales such as channel width or the Rossby radius of

deformation, and the extent of cross-stream motion is constrained by these scales, then the dynamics of nonlinear dispersion is generally governed by an equation of the KdV type (Section 1.9c). The long-wave limit in such cases can clearly be defined. A case in which this constraint is absent occurs if the wall at y=1 in the Figure 6.2.1 channel is moved to infinity. Although a long-wave approximation can still be defined for the fluid lying between the wall at y=0 and the potential vorticity front, it cannot be defined in the outer region. There the y scale is simply the x-scale associated with variations in Y. Such cases arise naturally in coastal applications and are governed by Denjamin-Davis-Acrivos (BDA) type equations (see Grimshaw 1987 and Grimshaw and Yi 1990). There is an extensive literature on this subject, much of it summarized by Johnson and Clarke (2001).

e) *Related Coastal Applications*

The geometry of a typical continental shelf and slope can be crudely approximated by the step topography in the above model if the wall at y=1 is moved to infinity (Figure 6.2.8a,b). The topographic wave in this limit decays away from the step in the offshore direction. If an opposing uniform current is added, the waves can be arrested and hydraulic behavior similar to that discussed above can arise. A more realistic current, first proposed by Niiler and Mysak (1971), takes the form of an along-shore jet with piecewise uniform shear (Figure 6.2.8c). The jet velocity goes to zero at some offshore location and the ocean is considered quiescent further offshore. There are now two potential vorticity fronts, one associated with the topographic step and one associated with the offshore front. As shown by Niiler and Mysak, the flow has two wave modes, the first being a 'shelf' wave that shares features with the topographic waves discussed in the above channel model. The propagation speed of this wave may be positive or negative depending on the speed and frontal configuration of the jet. As shown by Collings and Grimshaw (1980), supercritical jets tend to be narrow and subcritical jets tend to be wide, as measured by the distance between the coast and either potential vorticity front. The second mode is a 'shear' wave that depends on the existence of the offshore potential vorticity front. It propagates in the same direction as the jet regardless of the parameter settings.

The shelf wave is special case of a general class of coastal trapped waves that owe their existence to the presence of the topographic potential vorticity gradients associated with continental slopes and shelves. In the absence of a background flow, the potential vorticity of the fluid increases towards the coast and Northern Hemisphere waves propagate keeping high potential vorticity (shallow water) on their right, i.e. in the same direction as a coastal Kelvin wave. Hydraulic behavior with respect to these waves can occur in the presence of an opposing flow. Hughes' (1986b) investigation of the Niiler and Mysak model confirms that the two conjugate states can occur for a given flow rate. The first is a relative wide, subcritical jet that allows upstream propagation of shelf waves; the second is a narrower and higher speed supercritical jet that carries shelf waves downstream. The shear wave does not appear to be directly implicated in the hydraulic behavior. However, instability can result from a resonance between the waves that can occur in the supercritical regime when their speeds become equal. It is also suggested

that transitions between the two regimes can occur as a result of changes in the shelf position, as was documented in coastal model discussed in Section 4.2.

Similar behavior can be found if the topography and potential vorticity vary continuously (Hughes 1985a, 1986a and 1987). If the coastline is aligned with the y^*-axis (north and south) then the cross-shelf (x^*) structure of a homogeneous flow is governed by

$$\frac{\partial}{\partial x^*}\left(\frac{1}{d^*}\frac{\partial \psi^*}{\partial x^*}\right) - d^* q^*(\psi^*) = -f \ , \qquad (6.2.16).$$

where ψ^* is the transport stream function ($v^* d^* = \partial \psi^* / \partial x^*$) and the full depth d^* is determined by the specified bottom topography. The solution procedure for the second order equations is to choose a potential vorticity distribution $q^*(\psi^*)$ and assign a particular value of ψ^* to the coastline. A value of $\partial \psi^* / \partial x^*$ at the coast is then guessed and (6.2.16) is integrated in positive x^* until v^* vanishes. The corresponding value of x^* is then considered the offshore edge of the current and fluid further offshore is assumed to be at rest. A series of similar calculations with different coastal values of $\partial \psi^* / \partial x^*$ yields a family of solutions with different widths and different transports. However, it is possible to find two or more solutions with the same volume transport. Hughes has shown how pairs of solutions with the same transport may be identified as conjugate states having the same transport and energy (see Exercise 7).

Although these flows are typically forced by along-shore changes in bottom topography, it is also possible to force the current by allowing the value of f to change. For a northwards (Northern Hemisphere) flow with the coast to the left (or southwards flow with the coast to the right) the increasing value of f causes subcritical and supercritical conjugate states to approach each other, possibly merging and becoming hydraulically critical at a particular latitude. However, unlike forcing due to topographic variations, the value of f does no reach a maximum value at the critical latitude but continues to increase in the northward direction. The solultions cease to exist beyond this latitude, suggesting that the flow separates from the coastline (Hughes, 1989).

Exercises

1. Derivation of the linear dispersion relation (6.2.1).

(a) Consider a channel with depth mean depth D and variable topography $h=h(y)$. Show that weak motion about a state of rest is governed by the topographic Rossby wave equation:

$$\frac{\partial}{\partial t}\nabla^2 \psi + \frac{\partial \psi}{\partial x}\frac{dh}{dy} = 0$$

in the nondimensional units used above.

(b) For a traveling wave with form $\psi = \mathrm{Re}[\Psi(y)e^{ik(x-ct)}]$ find the equation governing the cross-channel structure function $\Psi(y)$.

(c) Now suppose that dh/dy=0 accept near the channel midpoint y=1/2, where h changes abruptly from 1 to zero with increasing y. Using the result obtained in (b) show that

$$\left[\frac{d\Psi}{dy}\right] - \tfrac{1}{2}[h] = 0$$

where the brackets denote the change in the indicated quantity across the step.

(d) Write down the separate solutions for $\Psi(y)$ in the regions to the north and south of the step, apply the boundary conditions at the channel walls, and match the solution using the result in (c) and the requirement that $\Psi(y)$remain continuous across the step to obtain the dispersion relation

$$c = \tfrac{1}{2}k\tanh\left(\tfrac{1}{2}k\right)$$

and deduce the result by (6.2.4) by adding a background velocity -a and dimensionalizing.

2. Consider the linear dispersion relation (6.2.4) for the case when the step and front lie at mid-channel. According to (6.2.4) long waves are brought to rest when $\alpha^*=1/4f_o w^*\delta h^*/D$. Try to obtain a similar estimate using the dispersion relation for waves in a channel with a constantly sloping bottom. [A good place to start is to write down a version of (2.1.30), altered to account for a mean flow and a rigid lid.]

3. Show that equation (6.2.5) is invariant to the change in variables $\hat{y} = 1 - y$, $\hat{Y} = 1 - Y$, and $\hat{Y}_h = 1 - Y_h$. Using the fact that the initial condition Y=Y_h is also invariant, conclude that if $Y(x,t)$ is a solution than 1- $Y(x,t)$ is also a solution for the case in which the position of the step is reflected about the channel axis (y=1/2). By this means the solutions shown in Figures 6.2.4-6.2.7 can be used to construct the solution to for the case in which the shelf width increases rather than decreases.

4. Show that for $Y>Y_\mathrm{h}$, the characteristic speed is given by $c = -\alpha - \tfrac{1}{2}[3Y^2 - 2Y + Y_h^2]$. Note the corresponding Froude number formula $F_o = -2\alpha / [3Y^2 - 2Y + Y_h^2]$. Show that an upstream disturbance which increases the value of Y over its undisturbed value 0.5 must be a rarefaction.

and an upstream disturbance that increases Y_∞ above its initial value (=0.5) is a rarefaction.

5. Show that the value of the potential $V(Y,Y_h)$ is the same at the two supercritical fixed points in Figure 6.2.7a. [This result can be used as the basis for a matching condition across a supercritical leap, as discussed by Johnson and Clarke (1999)]

6. Using a contouring routine, construct a phase plane diagram akin to Figure 6.2.7 for the case Y_h=.55, α=1, and with the upstream position of the front located at the step (ψ_o=.055). Show that the two supercritical fixed points are no longer connected and, instead, there is a closed (*homoclinic*) trajectory attached to one of these points. Describe the associated solution. Draw a sketch showing the shapes of the stationary waves associated with the periodic orbits as the limiting homoclinic orbit is approached. *(The phase plane is Figure 6c of John and Clarke, 2001)*

7. Suppose that two distinct solutions to (6.2.16) are found for the same potential vorticity distribution and topography. Both have the same transport and both can be smoothly joined to a quiescent region far offshore. Show that the distribution of the Bernoulli function along streamlines is the same in each case.

Figures

6.2.1 Definition sketch.

6.2.2a-h Four realizations of the solution space Y vs. Y_h for different background flows: (a): α=.05, (c): α=.1, (e): α=.15, (g): α=.3. The bold overlaying curves show steady solutions for the case ε=0.15 and for the initial value Y_∞=0.5. These solutions are shown in plan view in the frames immediately to the right. (Figure 2 from Johnson and Clarke, 1999.)

6.2.2i An enlarged version of frame (e) of the previous figures. The dashed curve shows the nominal (and incorrect) solution that one would obtain by assuming critical flow at the section of minimum shelf contraction. The solid curve and arrows shows the solution with a supercritical leap.

6.2.3 The regimes of steady, long wave solutions in terms of ε and α, all assuming the initial value Y_∞=0.5. (Based on Figure 9 of Haines, et al. 1993.)

6.2.4 Contour dynamical solutions of the full barotropic equations for α=1/6π and ε=1/8. Frames (a) and (b) use obstacles of different lengths. The position of the topographic step is shown as a dashed line, the predicted long wave solution by a thick solid line, and the CD solution by a thin and solid line. (a): $\mu^{1/2}=\pi/(32)^{1/2}$ and t=102. (b): $\mu^{1/2}=\pi/2$ and t=42. Note x and t are the primitive, not the stretched, versions. (Figure 4 or Haynes, et

al. 1993). *Note: the values of ε quoted by HJH are twice the values of ε as defined by JH. Since I am basing my discussion on JH, cut the quoted HJH values in half. $\alpha=1/6\pi$ and $\varepsilon=1/8$ in both cases.*

6.2.5 Figure 6 of HFH. Same as Figure 6.2.4 accept that ε has been increased to 1/4.

6.2.6 Development of an approach control with a supercritical leap. The parameters are the same as in Figure 6.2.5a, but α has been increased to $1/3\pi$. (a) The front at three time intervals intervals up to t=18. The dashed curve indicates the position of the step and the initial position of the front. (b) The front (thin solid line) at t=26.5 has developed an abrupt bend just upstream of the contraction. Shown by thick solid line is a version of the steady, approached controlled, long-wave solution (dashed line) in which the supercritical leap occurs at the first opportunity. (c) By t=77.5 the abrupt bend in the front has moved downstream of the contraction and has settled into a steady state supercritical leap. (Based on Figure 11 of Haynes, et al. 1993)

6.2.7 (a) Phase plane trajectories for (6.2.15) with Y_h=0.5, α=0.1, and $\psi_o=\alpha/2$. (b) The solution corresponding to the dashed trajectory of (a). (Figure 6 of Johnson and Clarke, 2001).

6.2.8 Step approximation (a) to a typical shelf topography (b). Plan view of the coastal jet considered by Niiler and Mysak (1971).

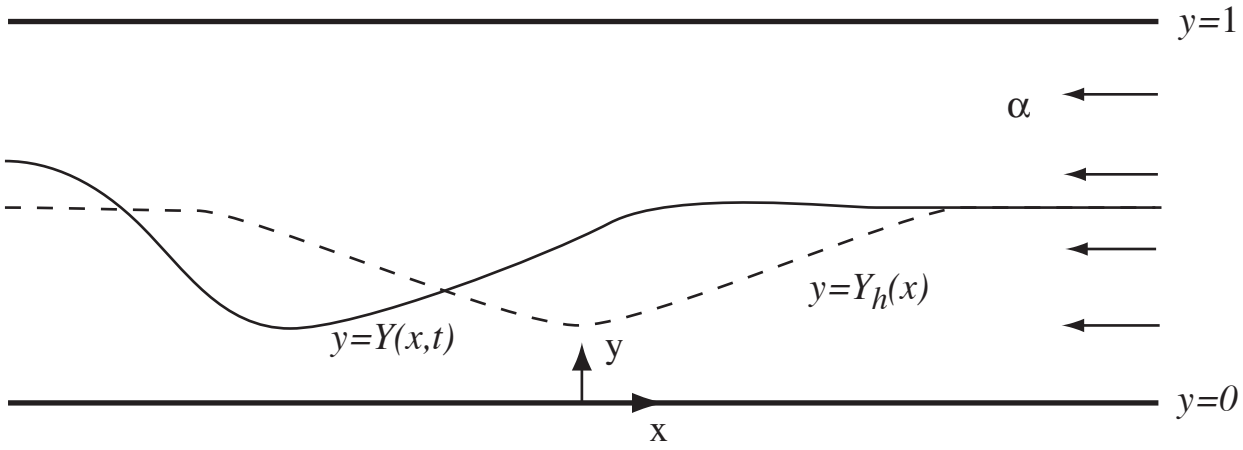

(a)

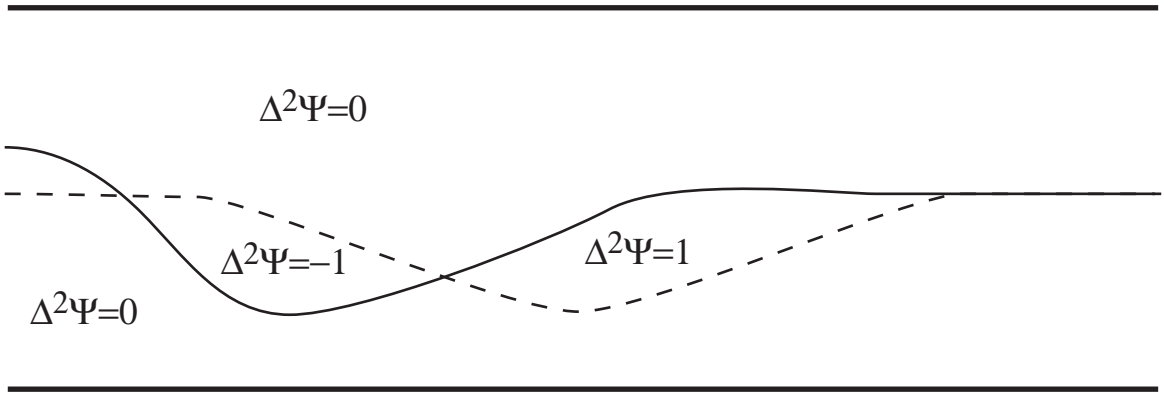

(b)

Fig. 6.2.1

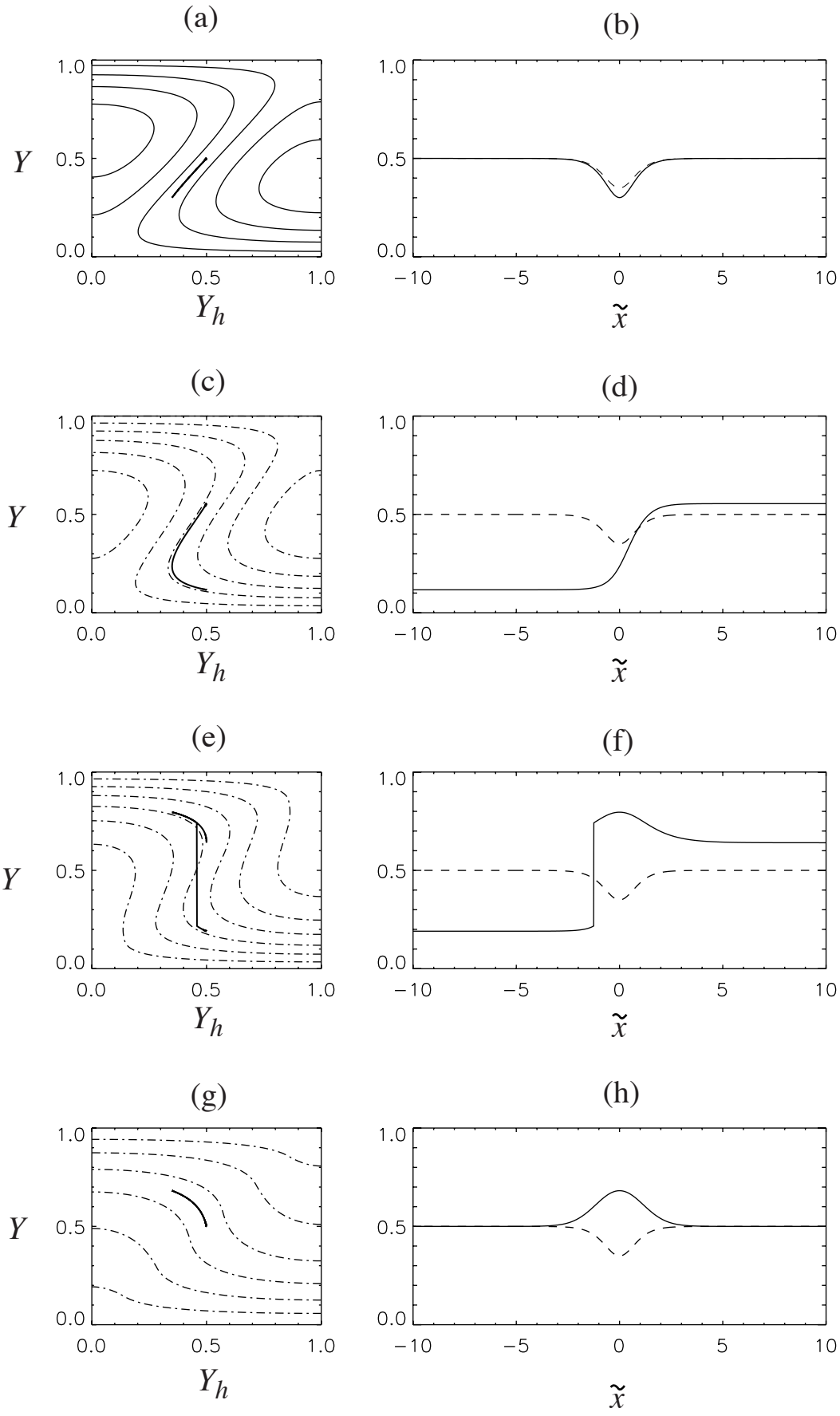

Figure 6.2.3

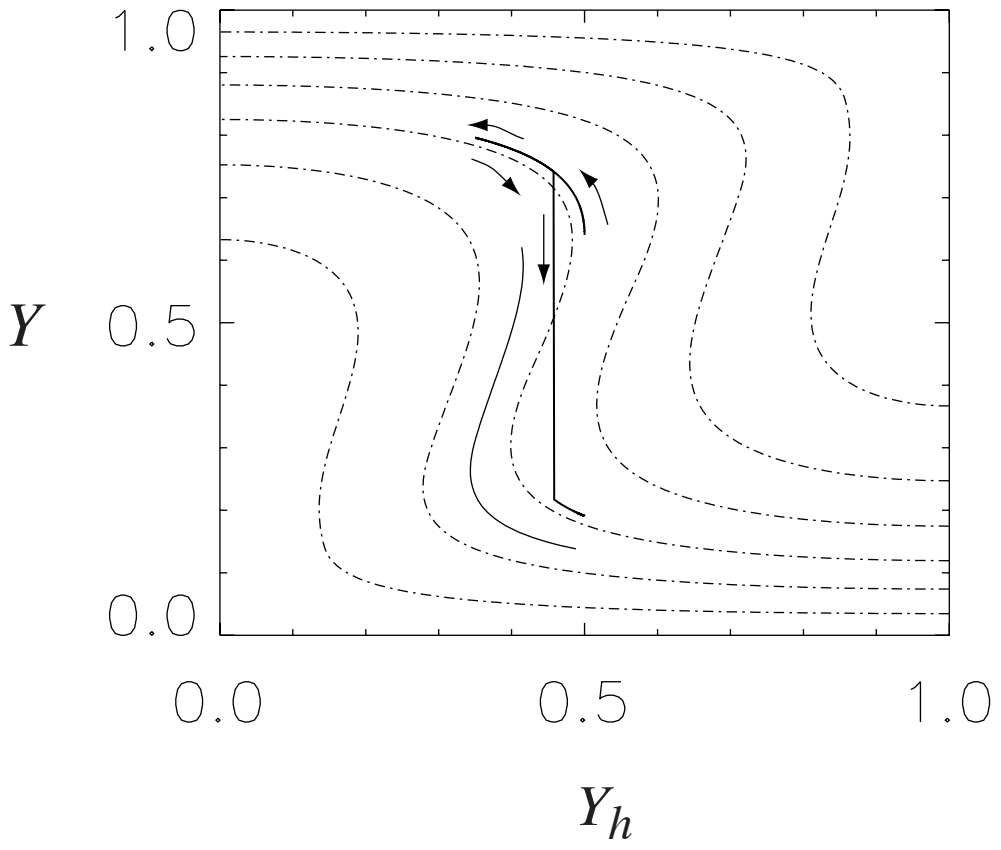

Figure 2.6.2i

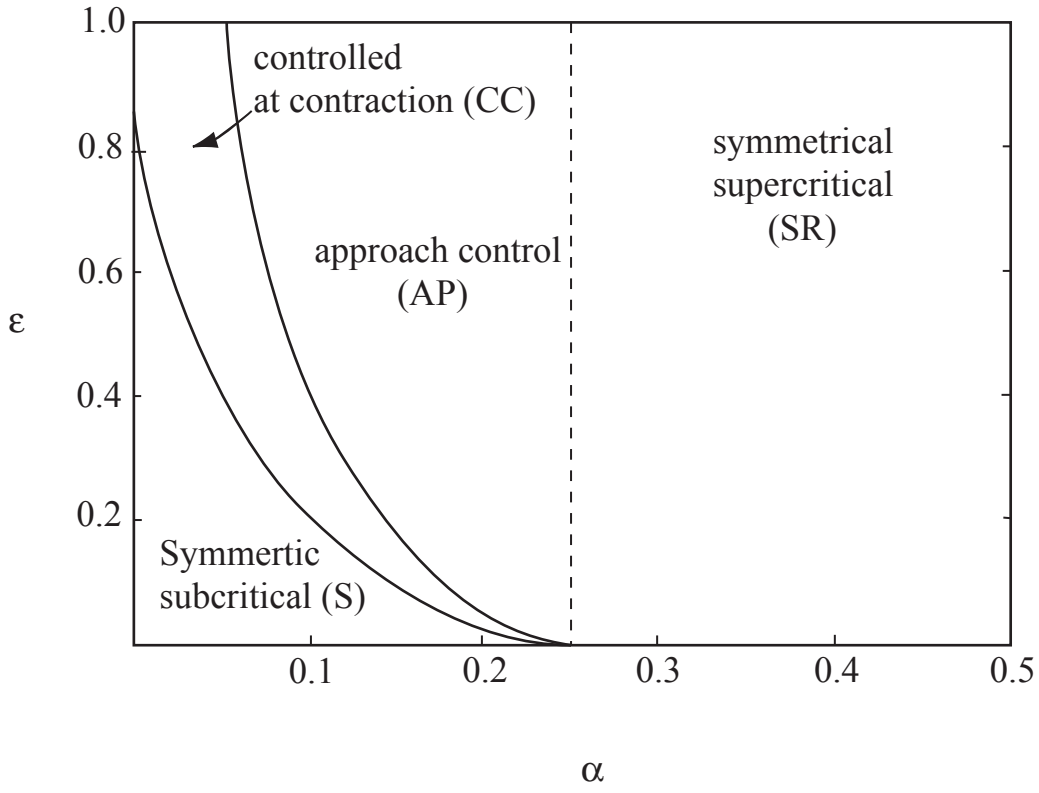
1.0
0.8
0.6
0.4
0.2
ε
controlled
at contraction (CC)
symmetrical
supercritical
(SR)
approach control
(AP)
Symmertic
subcritical (S)
0.1
0.2
0.3
0.4
0.5
α

Figure 6.2.3

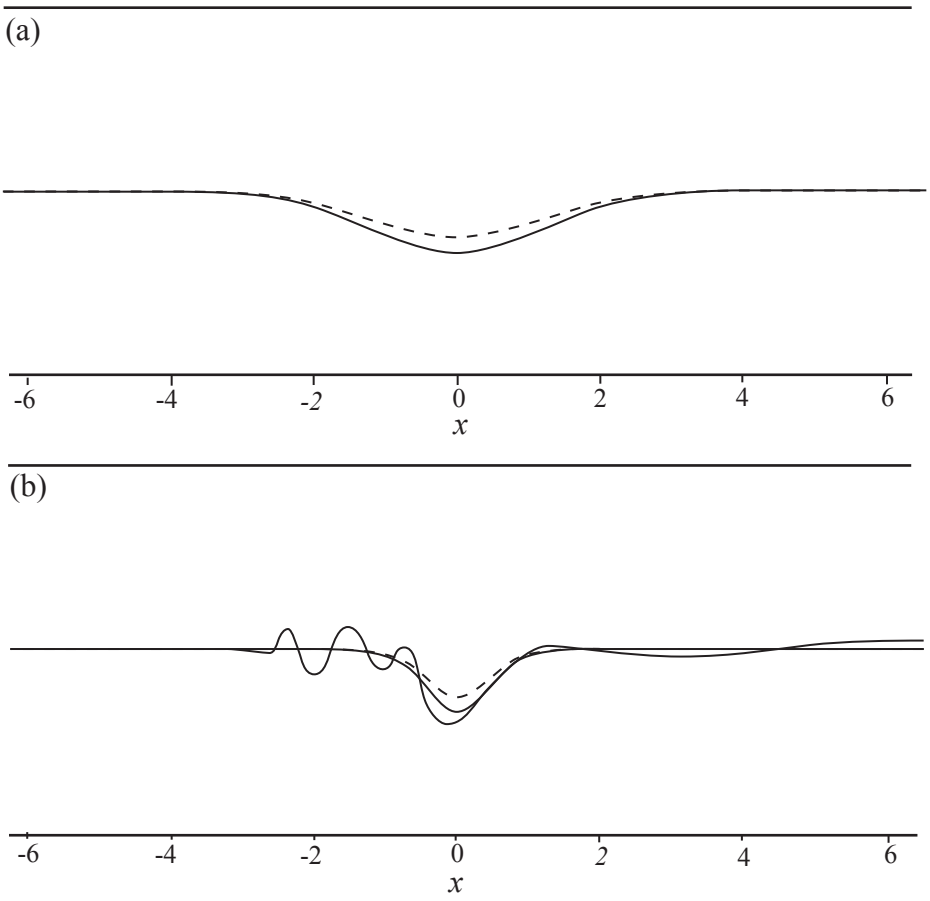

Fig. 6.2.4

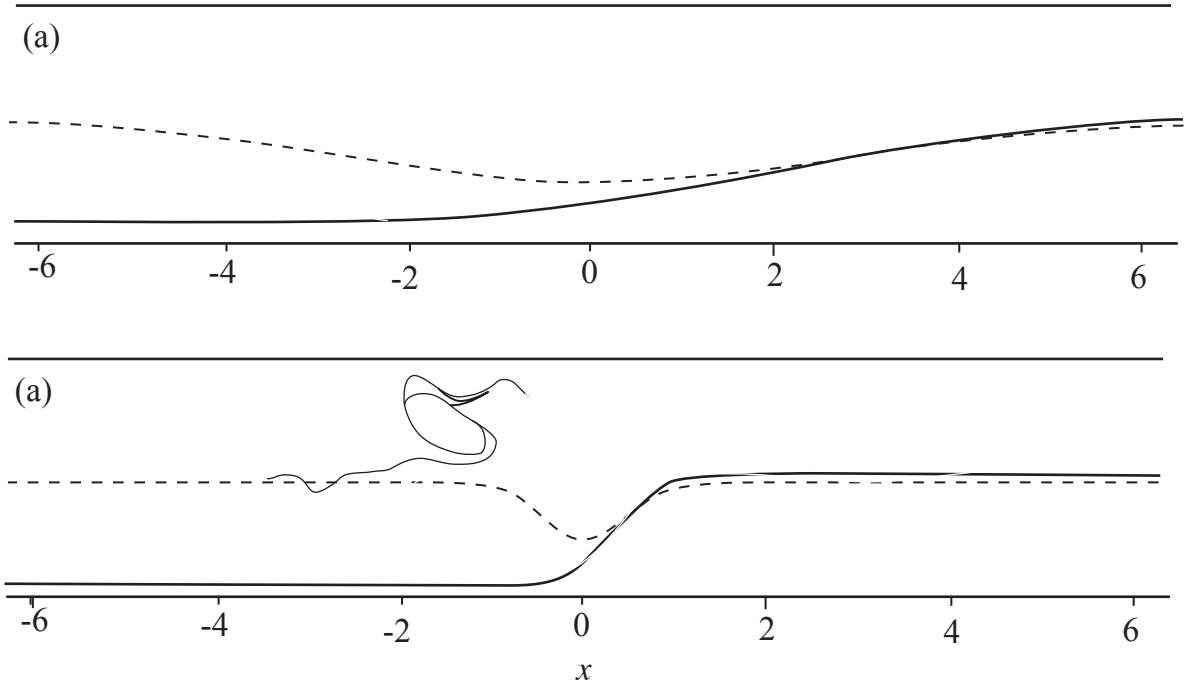

Figure 6.2.5

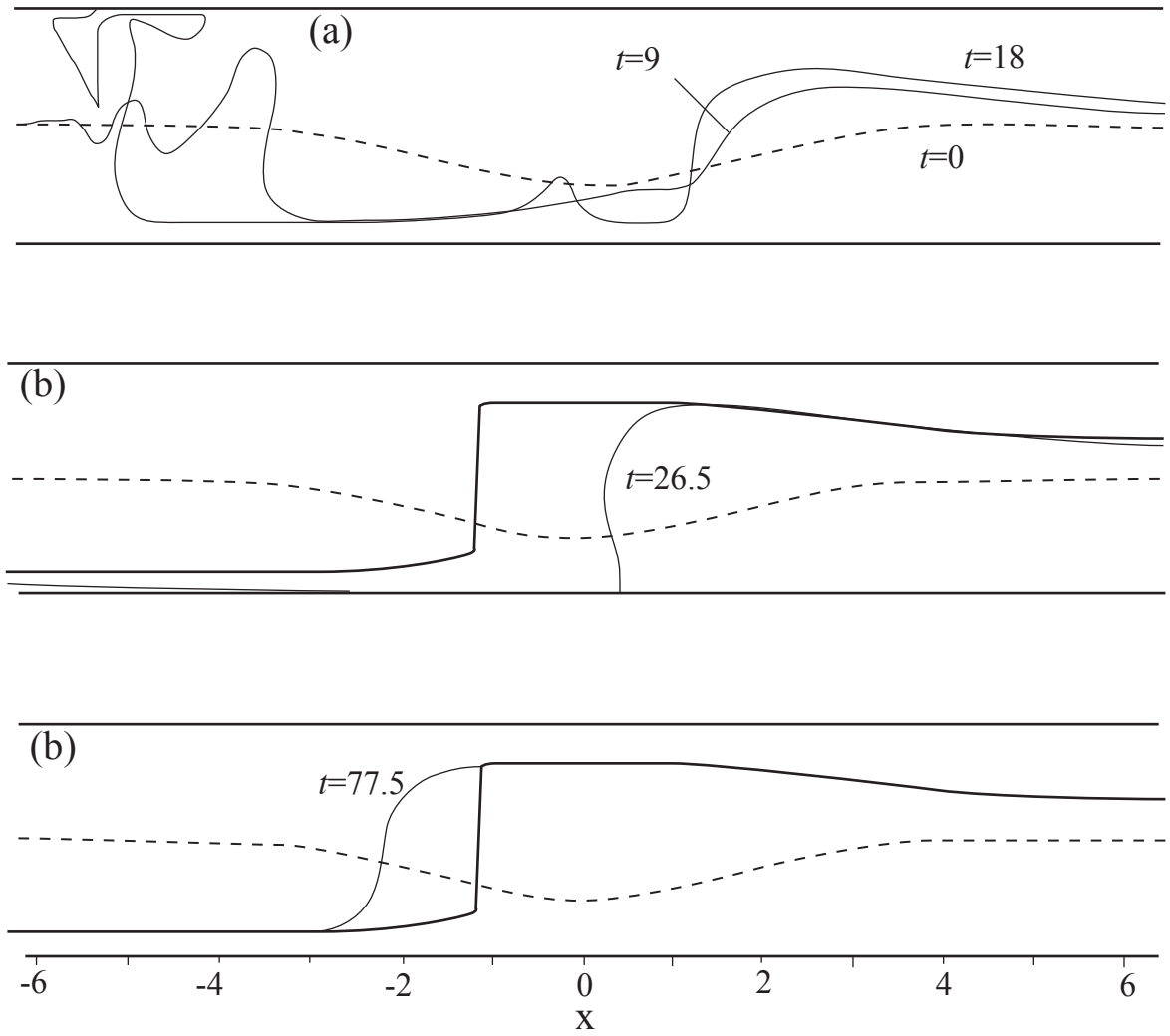

Figure 6.2.6

(a)

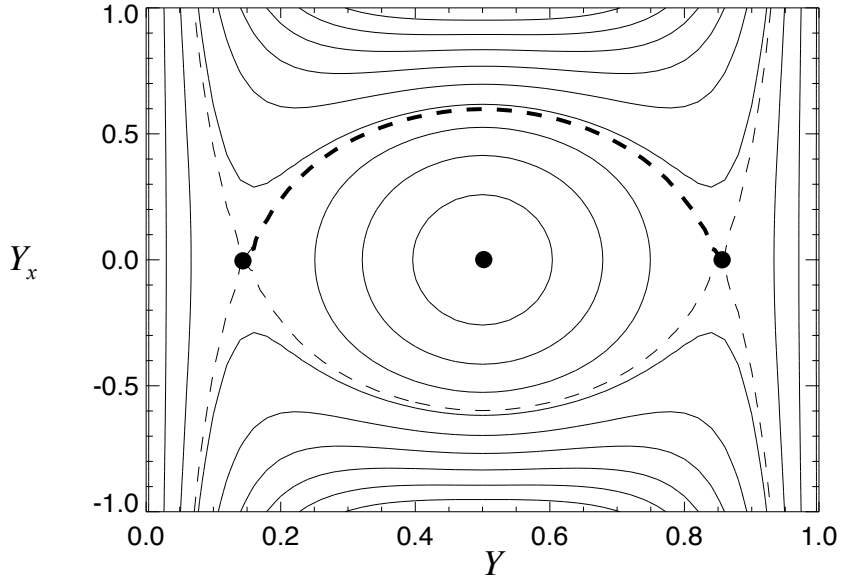

(b)

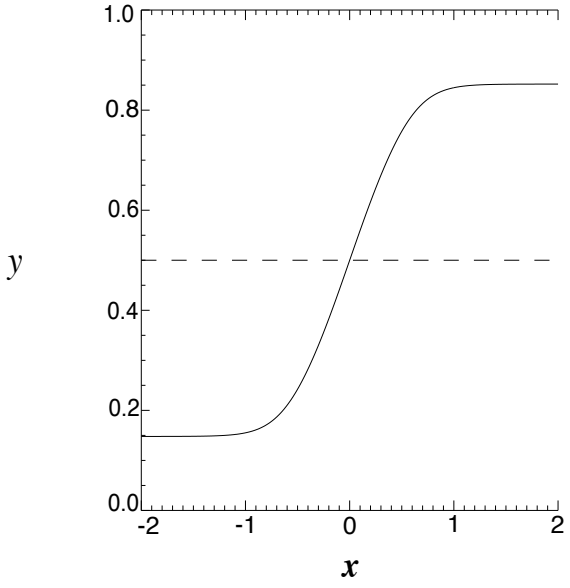

Figure 6.2.7

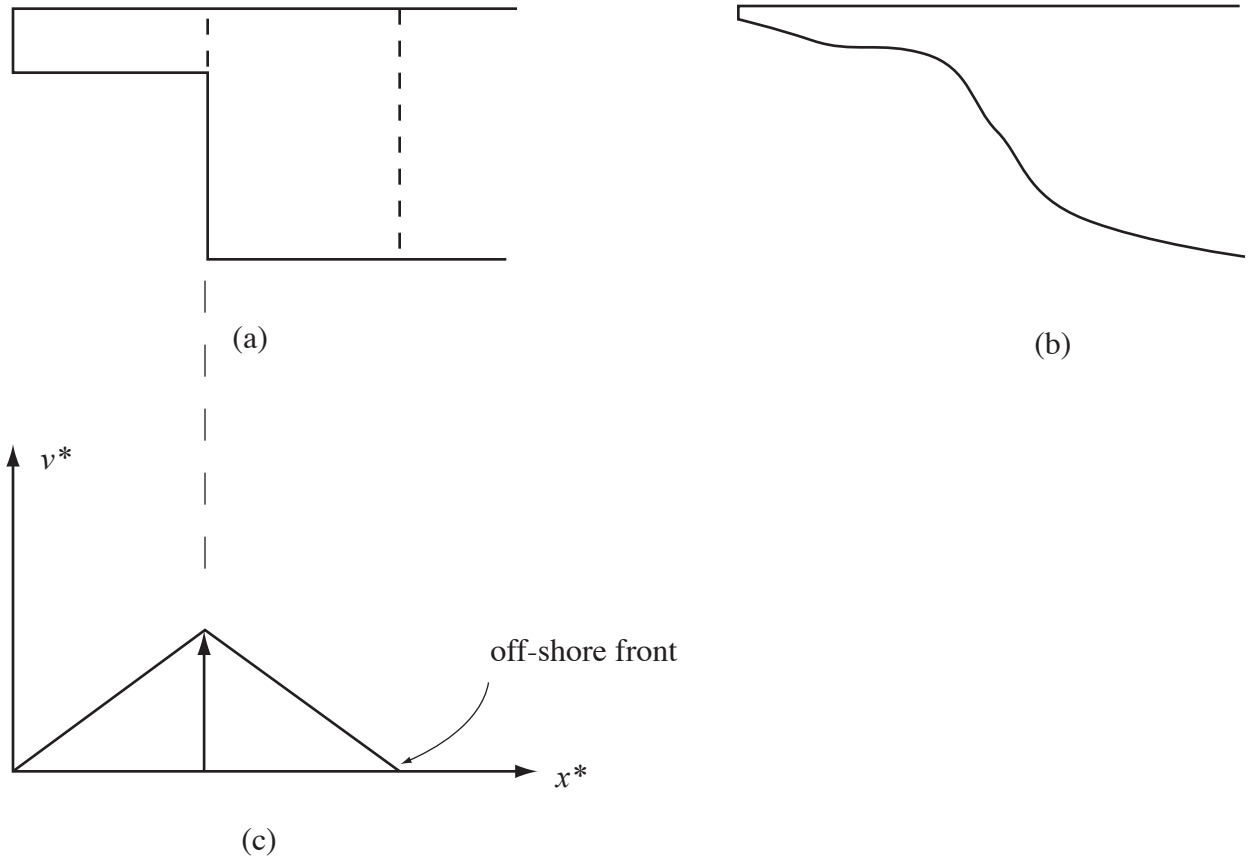

Figure 6.2.8